DOE/ER/13942--3

DE92 000834

Final Progress Report

September, 1986 - June, 1991

DOE/ER/13942-3

PHOTOINDUCED CHARGE SEPARATION BY POLYMER-BOUND CHROMOPHORES

Dr. Michael A. J. Rodgers
Center for Photochemical Sciences
Bowling Green State University
Bowling Green, Ohio 43403

September, 1991

PREPARED FOR THE U. S. DEPARTMENT OF ENERGY
UNDER GRANT NUMBER DE-FG02-88ER13942

DISCLAIMER

FINAL PROGRESS REPORT

1.0 Project Overview

A major thrust of the project has been to examine the photodynamic behavior of water-soluble polymers that have covalently linked hydrophobic chromophores spaced along the chains. These polymeric systems have been examined for photoinduced charge separation with electron-accepting ions having different total charge. Focus has been on the excited singlet (S_1) state formed by laser flash absorption. The effects of pH and ionic strength -- factors that govern the conformational nature of the polymer in solution -- have been studied. A second major effort has been to study photoinduced redox processes involving excited states of water-soluble variants of anthracene and acridine.

2.0 First Two Program Years

The molecules that have been studied are shown in Scheme 1. The polymer chain has been polymethacrylic acid (PMA); and the pendant chromophores have been diphenylanthracene (DPA), anthracene (A) and its ethyl (EA) and 10-phenyl (PA) derivatives, pyrene (PY), perylene (PER), and an amino-naphthalimide (ANI). Excited state quenchers that have been used are N,N'-dimethylbipyridinium cations (methylviologen, MV) and N,N'-disulfonatopropylbipyridinium zwitterions (SPV) and N,N'-sulfonatopropylmethylbipyridinium cations.

2.1 Fluorescence Quenching and Charge Separation Studies

Upon photoexcitation the bound chromophores have a strong tendency to undergo radiative deactivation, much as the free model chromophores do. The results of quenching this fluorescence with the viologens stated above have been described in detail in recent publications (Appendices I through IV), and only the major conclusions will be presented here:

(i) Fluorescence quenching occurs by a mixture of static and dynamic mechanisms.

(ii) The nature of the quenching depends on the pH of the aqueous medium since at high pH the polymer is deprotonated and exists as an extended chain polyelectrolyte. At low pH (2.8) the polymer backbone is protonated, which causes the polymer to coil, thus providing a mix of hydrophobic and hydrophilic regions.

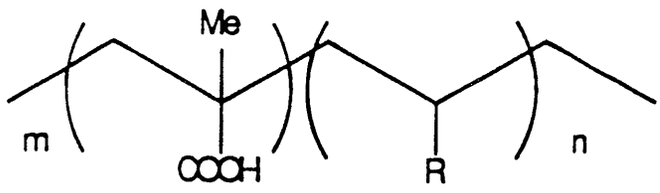

Polymethacrylic acid (PMA)

R =

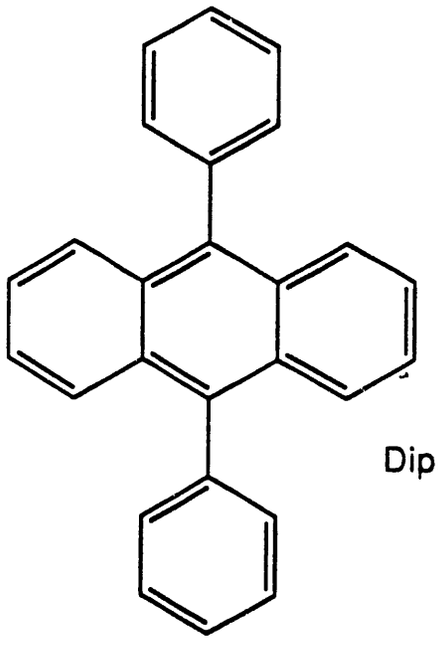

Diphenylanthracene

R =

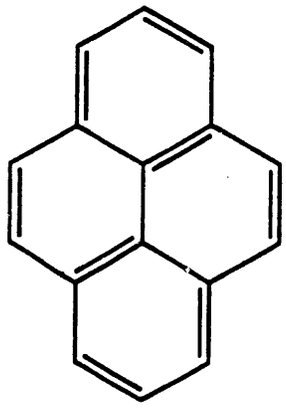

Pyrene

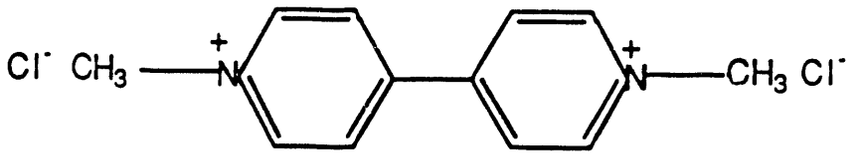

Methylviologen Dichloride

Scheme 1.

(iii) The viologen quenchers can form a charge transfer complex with the aromatic chromophores when the polymer is extended.

(iv) The equilibrium constants for both static association and charge transfer complexation fall as the steric hindrance by residues attached to the anthracene nucleus increases.

(v) At high pH, excitation of the chromophore (at 355 nm) in the presence of viologens in sufficient quantity to show strong fluorescence quenching behavior resulted in no appearance of aromatic radical cation-viologen cation ion pairs at times longer than *ca* 100 ns.

(vi) At pH = 2.8, for the anthracene derivatives and for perylene, high yields of photoinduced charge transfer products were observed at times corresponding to hundreds of ns post laser flash. Quantum yields varied over the range of 0.3 to 0.45. For ANI such yields were significantly less. With PMA-PY, no ion separation was observed at high or low pH.

(vii) When formed, the decay of the charge-separated species was slow enough for them to persist for milliseconds.

Table I summarizes the charge escape data:

Table I. Charge Escape Yield and Back Reaction Rate

	MV^{2+}		SPV	
polymer[a]	ϕ_{ce}	k_{cr} ($\times 10^{-9}$ $M^{-1}s^{-1}$)	ϕ_{ce}	k_{cr} ($\times 10^{-9}$ $M^{-1}s^{-1}$)
PMA-A	.32	1.5	.41	3.1
PMA-EA	.41	1.2	.35	4.2
PMA-PA	.41	1.1	.44	2.0
PMA-DPA	.40	2.0	.30	1.6
PMA-PY	~0	---	~0	---
PMA-PER	.36	21	.41	8
PMA-ANI	.07	9	.18	11

a. See Scheme 1 for structures.

22 Matters Arising from Fluorescence and Charge Separation Studies

While much interesting data had been gained from the fluorescence and charge-separation studies, the results pose more questions. The major feature that had been established was that photoexcitation of chromophores attached at low doping (*ca* 1%) to water-soluble polymers in some cases leads to significant yields of charge-separated species. Moreover, these ions have lifetimes of some milliseconds, governed by bimolecular radical-radical annihilation.

What is not yet revealed is:

(i) Whether the charge separation process was derived from the S_1 or T_1 states of the chromophore. Certainly ion production was only observed at concentrations of acceptor that were necessary to significantly quench S_1, but we cannot yet discount a T_1 precursor since we have not examined the behavior of T_1 under the experimental conditions.

(ii) What is the reason for our inability to measure $\phi_{ce} = 1$ in all cases? In the experiments our time resolution was limited to *ca* 100 ns and the quoted yields (Table I) refer to that time. It is conceivable that the initial yields are indeed unity and some cage recombination occurs prior to our observation time.

(iii) Why the severe pH dependence? Clearly polymer conformational changes are occurring, but how do these affect the excited state-acceptor interaction? Again, could yields be high initially followed by total rapid decay at pH = 10?

(iv) Why should the anthracene derivatives differ so dramatically from pyrene? What are the molecular features that contribute, and is there again a temporal feature to be revealed?

Questions such as these have led us to seek information at shorter times after excitation. These studies have been conducted at Bowling Green in years 02 and 03 of the grant using instrumentation capable of making absorption spectral measurements at times as short as 20 ps.

3.0 **Program Years 2 and 3**

Since relocation to Bowling Green State University in January, 1988, the project has proceeded through an instrumentation construction and fine-tuning phase, and a research phase. These are described in the next sections.

3.1 Instrumentation

3.1.1 Picosecond Absorption Apparatus

A Quantel YG571C active/passive mode locked Nd:YAG laser operating at 5 Hz produces a 30 ps FWMH pulse of 1064 nm radiation. This is then amplified in a double pass 9 mm diameter Nd:YAG rod amplified to 75 mJ. The second harmonic (532 nm) and third harmonic (355 nm) are generated by passage of the fundamental through a second harmonic generator (SHG) and a third harmonic generator (THG) respectively. The beam output is now a mixture of 1064, 532 and 355 nm radiation.

Diagram 1 displays the optical arrangement for the picosecond absorption apparatus. The fundamental is separated from the third harmonic by dichroic mirror 1 (DM1). The fundamental is purified from the residual visible radiation by an IR transmitting filter F1. The 1064 nm radiation is reflected onto the delay prisms by an IR turning mirror (IRM). The position of the prisms is adjusted by a computer-controlled linear stepping motor riding on a 50 cm platen. This gives a usable delay between pump and probe pulses of approximately 3 ns. The fundamental is focused by lens L1 into a 10 cm cylindrical cell containing a 50/50 v/v mixture of D_2O/H_2O. The white light continuum generated by self-phase modulation has a probe range between 400-800 nm (see Figure 1). The continuum is picked up by a bifurcated fiber optic cable which produces I_t and I_o channels. The continuum is spatially filtered with a 300 μm pinhole and collimated with a micro-lens, to produce a probe (I_t) and a reference (I_o) beam of 1 mm diameter.

The second harmonic (532 nm) or the third harmonic (355 nm) serve as the excitation (pump) pulse which is focused into the sample cell with a cylindrical lens (L2). The fiber optic output cables pick up the continuum after passing through excited and unexcited regions of the sample and are dispersed onto an unintensified dual diode array with an SA HR320 spectrograph. Typically 400 laser shots are averaged to produce a spectrum with a good S/N ratio. Absorption spectra were calculated according to the following expression:

Diagram 1. Picosecond Absorption Apparatus

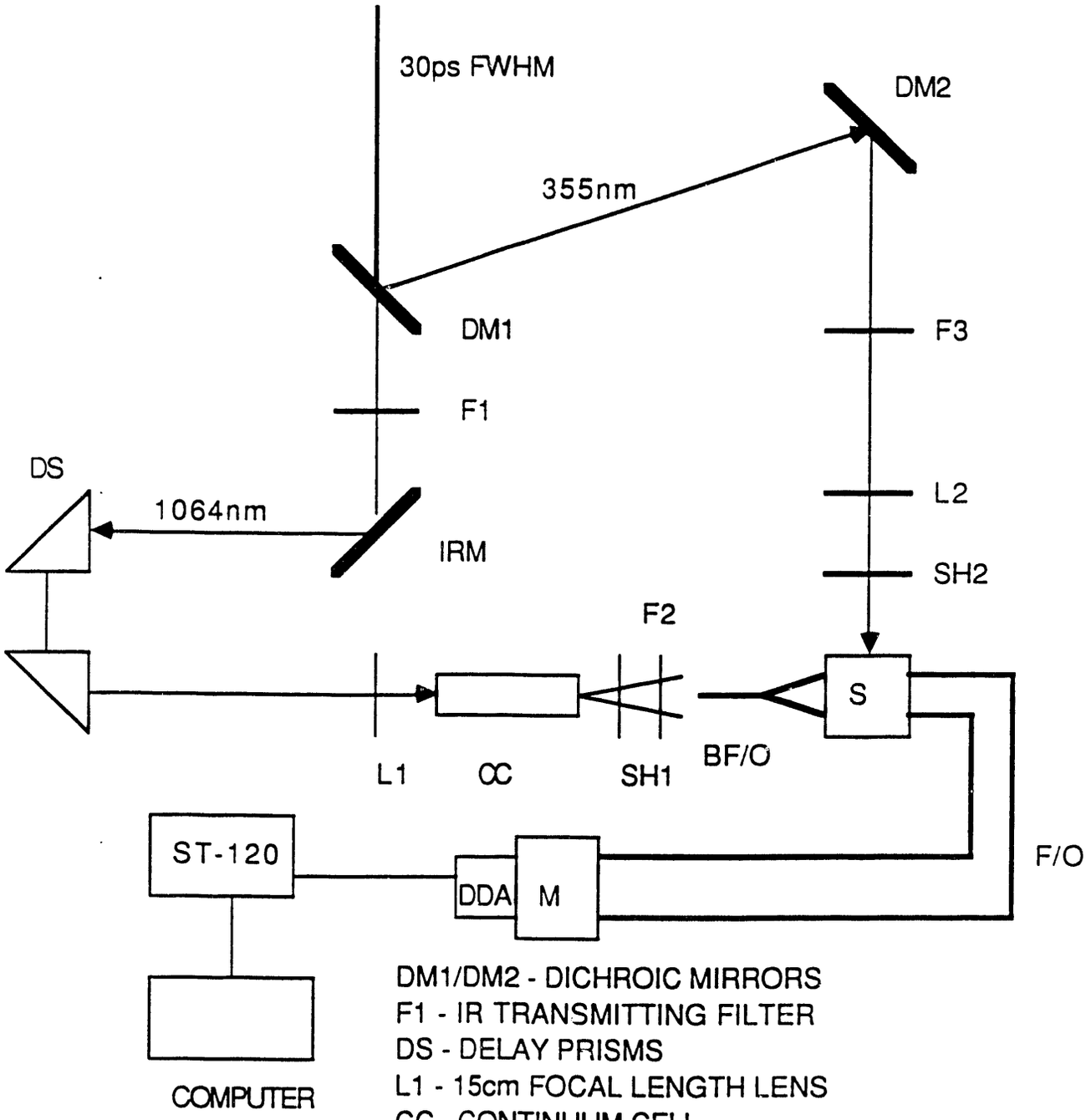

DM1/DM2 - DICHROIC MIRRORS
F1 - IR TRANSMITTING FILTER
DS - DELAY PRISMS
L1 - 15cm FOCAL LENGTH LENS
CC - CONTINUUM CELL
SH1/SH2 - SHUTTERS
BF/O - BIFURCATED FIBRE OPTIC
F/O - FIBRE OPTIC PICKUP
M - SPECTROGRAPH
DDA- DUAL DIODE ARRAY
ST-120 - DIODE ARRAY CONTROLLER
IRM - IR TURNING MIRROR
F2/F3 - BANDPASS/HEAT FILTERS
L2 - CYLINDRICAL LENS

Figure 1. Continuum Spectrum

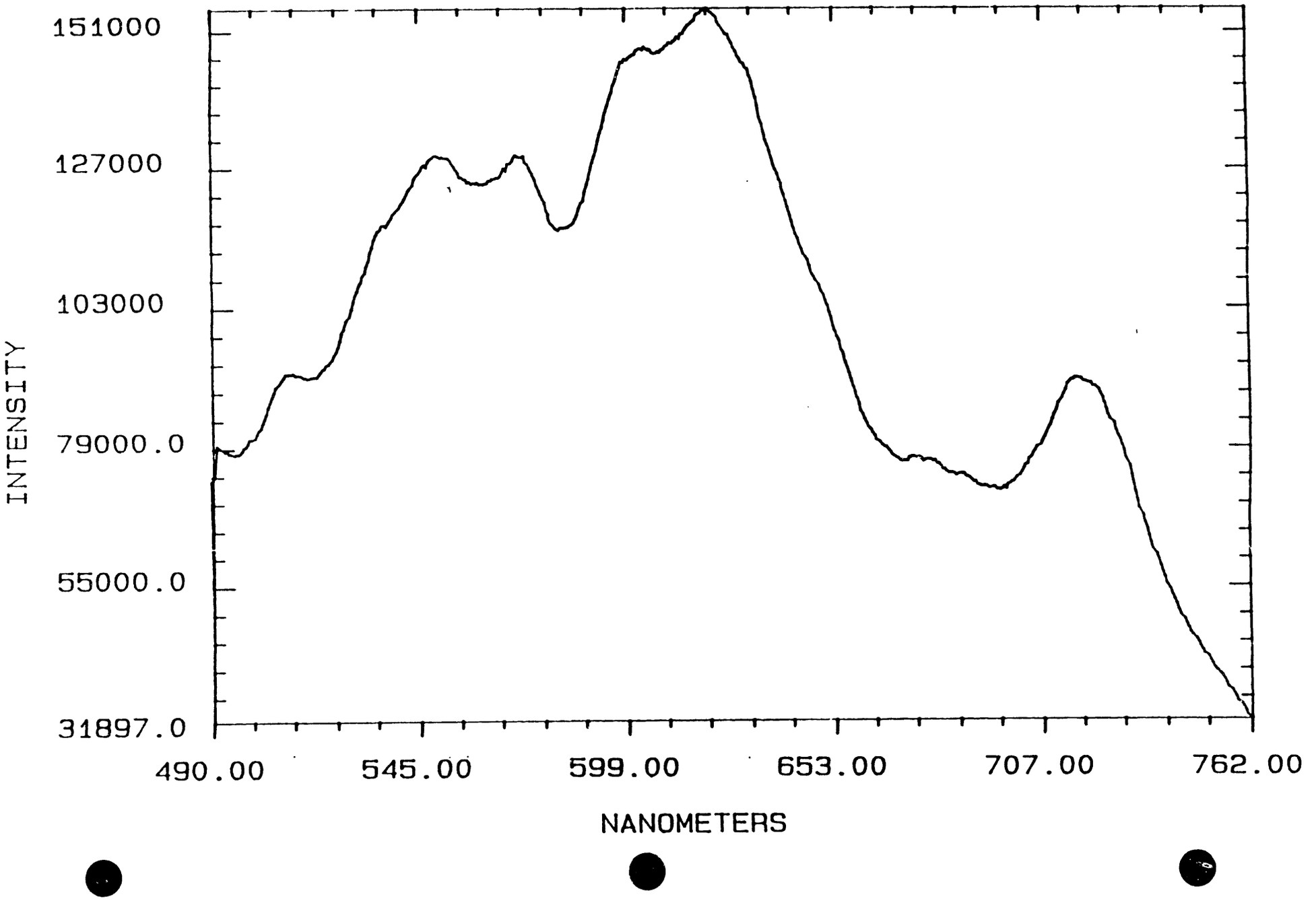

$$Abs = \log \left(\frac{I_t \times I_0^e}{I_0 \times I_t^e} \right)$$

where I_0, I_t, I_0^e, and I_t^e refer to reference and sample channels with and without excitation after dark-current subtraction. If the sample emits (e.g., fluorescence) in the spectral window of interrogation, this emission is subtracted from the continuum prior to the absorption calculation. This is accomplished by allowing the pump pulse to impinge upon the sample without the probe pulse, thus recording the emission spectrum.

Time zero was determined by monitoring the rise of the maximum of the $S_1 \rightarrow S_n$ absorption of 1,4-diphenyl-1,3-butadiene (DPB) excited at 355 nm, as a function of delay time. The time which corresponds to one half of the maximum absorption is defined as the origin of the time axis and corresponds to the maximum temporal overlap between pump and probe pulses. Figure 2 shows the rise and decay of the singlet absorption maximum (630 nm) of DPB. The response time of the apparatus is determined as the time required to go from 10% to 90% of the maximum, which in this case is 32 ps. A semilogarithmic plot of the absorption decay gave a singlet lifetime of 110 ps, which is in agreement with a previously reported value.[1]

3.2 Copolymer Preparation

Copolymers of methacrylic acid and vinyldiphenylanthracene (PMA-DPA) and pyrene (PMA-PY) were prepared as reported previously.[2] Structures of PMA-DPA and PMA-PY are shown in Scheme 1. Aqueous solutions of the copolymers were prepared with an optical density of 1.0 at 355 nm, which corresponds to a chromophore concentration of approximately 3.0×10^{-3} M for pyrene and 1.0×10^{-4} for DPA. The pH of these solutions was adjusted using NaOH and HCl. Polymer solutions were continuously flowed during photolysis in order to prevent the build-up of photoproducts. The flow rate was adjusted in order to ensure that the irradiated volume received no more than one excitation pulse. The energy of the excitation pulse was attenuated to ensure that no two-photon ionization of the chromophore occurred, followed by electron capture; i.e.,

$$D + 2\,h\nu = D^{+\bullet} + e^-_{(aq)} \qquad (1)$$

$$V^{2+} + e^-_{(aq)} = V^{+} \qquad (2)$$

Figure 2. Singlet absorption of DPB vs delay setting

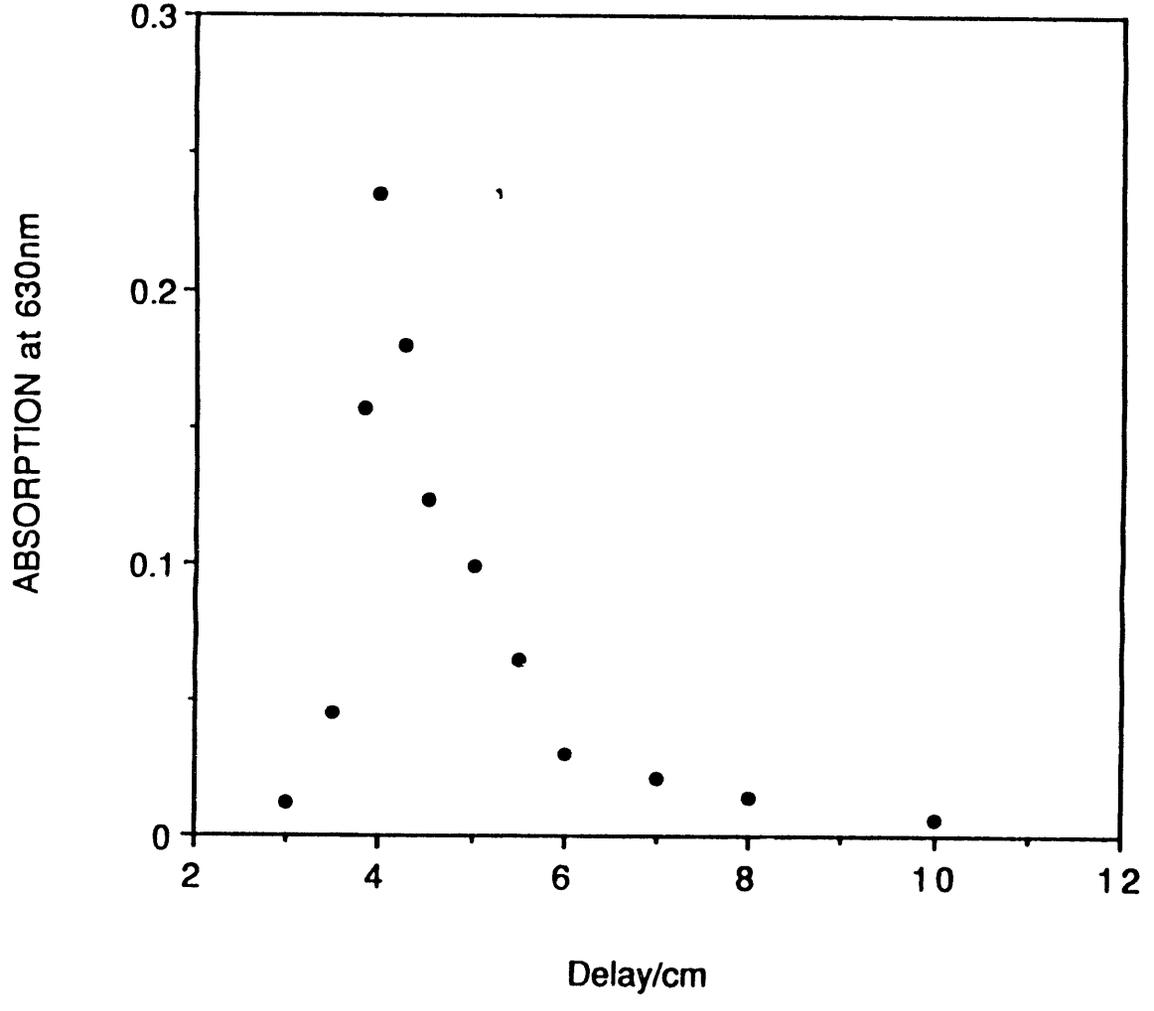

where D represents the aromatic chromophore and V^{2+} represents methyl viologen. Typically excitation energies were of *ca* 0.5 mJ. The area of the beam at the sample position was 0.4 cm^2.

3.3 Charge Separation Studies

3.3.1 PMA-DPA

Previous nanosecond studies of PMA-DPA have shown that efficient redox quenching of the DPA singlet can occur with viologens acting as electron acceptors. However, charge-separated products were only observed at low pH in high yields, *ca* 0.4, while at high pH no charge-separated products were observed.[2] Our new picosecond absorption spectroscopy data support these observations as follows:

PMA-DPA, pH = 2.8

The $S_1 \rightarrow S_n$ absorption of polymer-bound DPA in water at pH = 2.8 has its absorption maximum near to 572 nm, with little decay of S_1 state occurring over *ca* 3 ns (see Figure 3). Figure 4 shows the time profile of the $S_1 \rightarrow S_n$ absorption maximum. The time profile of the singlet absorption at 665 nm also follows a similar profile to that at 572 nm. Addition of 40 mM methylviologen (MV^{2+}) to the polymer solution quenches the S_1 state of DPA according to the following electron transfer reaction:

$$\text{(P)}\text{–}{}^1\text{DPA}^* + MV^{2+} \rightarrow \text{(P)}\text{–}\text{DPA}^{+\bullet} + MV^{+\bullet} \qquad (3)$$

Figure 5 shows absorption spectra obtained on the picosecond timescale after the addition of MV^{2+} to the polymer solution, which results in considerable broadening of the spectrum. This is attributed to the combined absorptions of DPA (S_1), $DPA^{+\bullet}$ and $MV^{+\bullet}$. Figures 6a and 6b show the time-dependent growth and slight decay of the absorption due to the $MV^{+\bullet}$ and $DPA^{+\bullet}$ radicals at 665 nm with the addition of 40 and 80 mM MV^{2+}. At 665 nm the $S_1 \rightarrow S_n$ absorption of DPA has no contribution.

These time profiles has been analyzed in terms of an exponential growth and decay which produces a reasonable fit (see Figures 6a and 6b). Table 2 displays the relevant parameters obtained from a nonlinear least-squares fitting routine. The rate of growth of the absorption at 655-nm appears to be independent of viologen concentration.

Figure 3 . PMA-DPA. pH=2.8. singlet absorption.
Delays: (a) -80 (b) 53 (c) 1085 (d) 2417ps

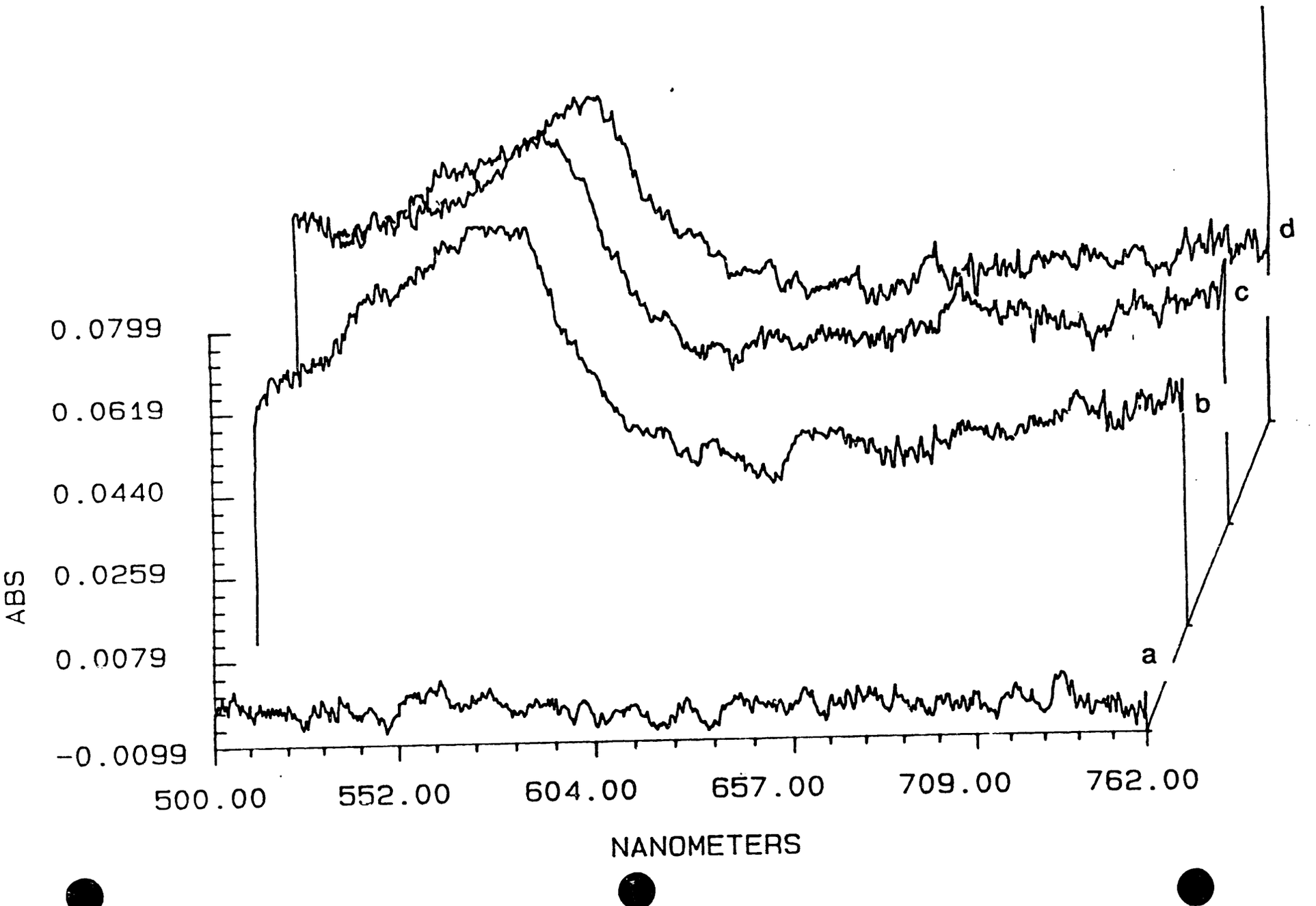

Figure 4. PMA-DPA, pH=2.8. Singlet absorption decay.

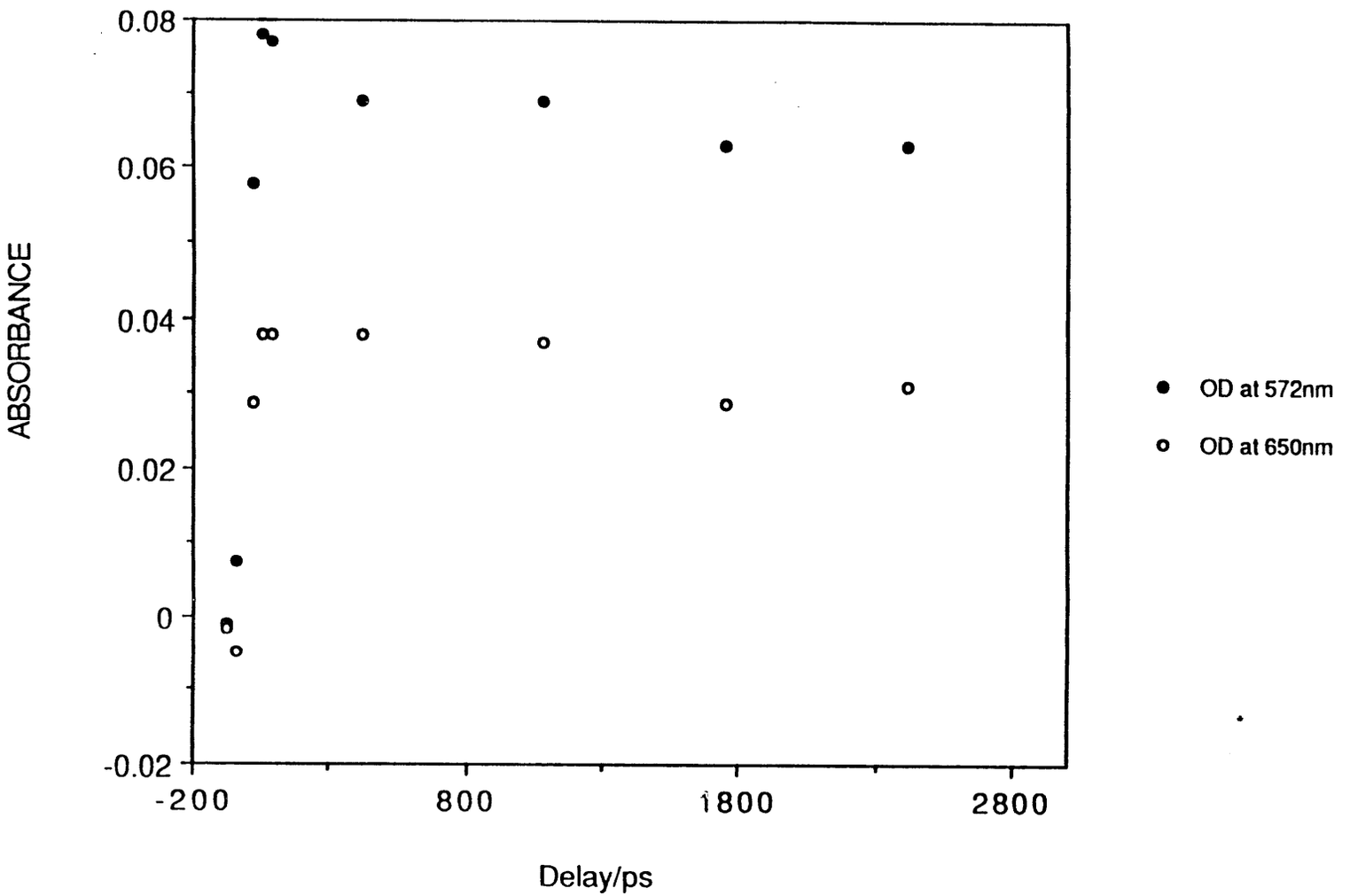

Figure 5 PMA-DPA, pH=2.8, [MV2+] =80mM

Delays: (a) -46 (b) 2817 (c) 1085 (d) 153ps

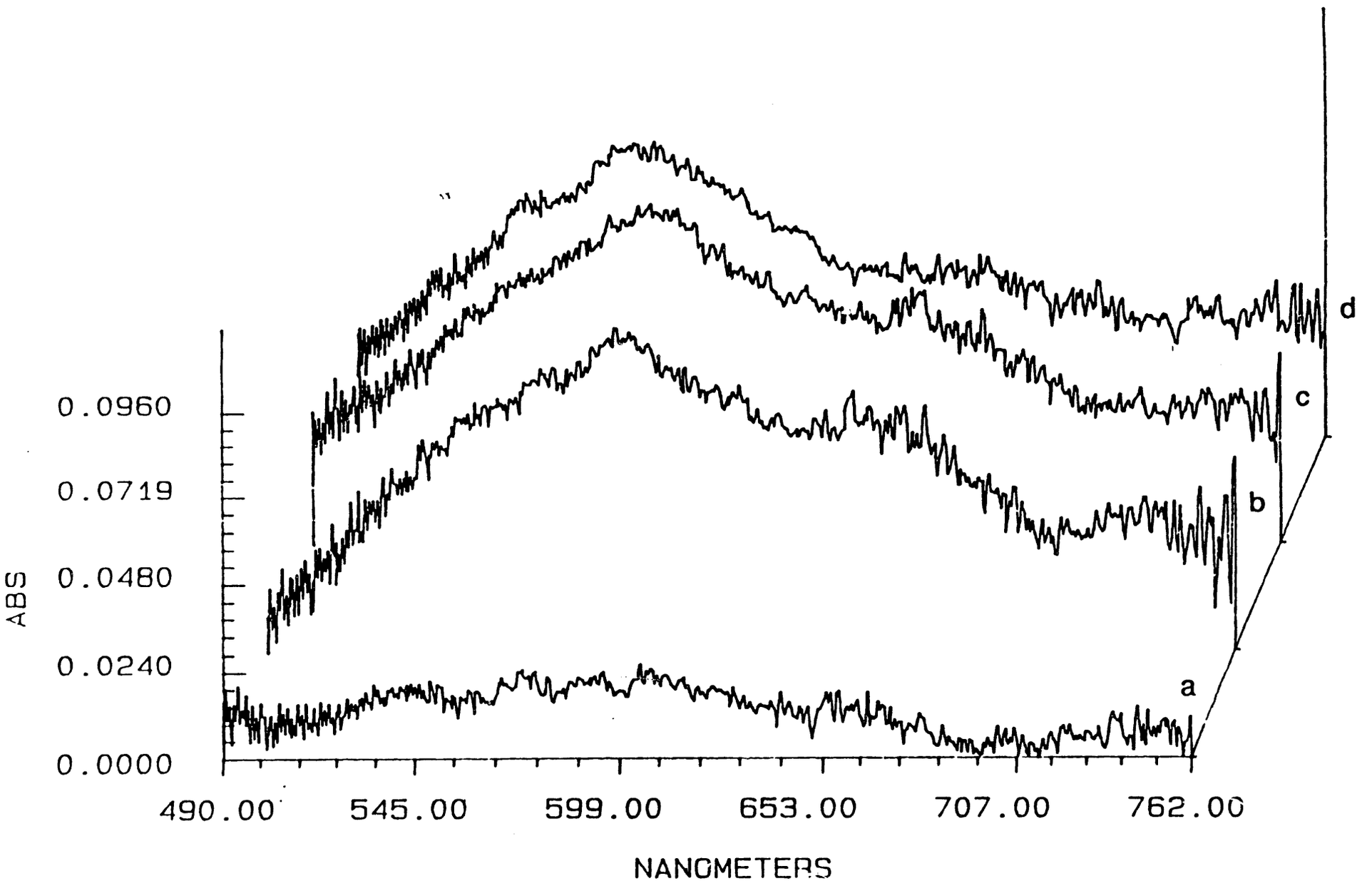

Figure 6a. PMA-DPA, [MV2+]=40mM, pH=2.8, fitted absorption rise.

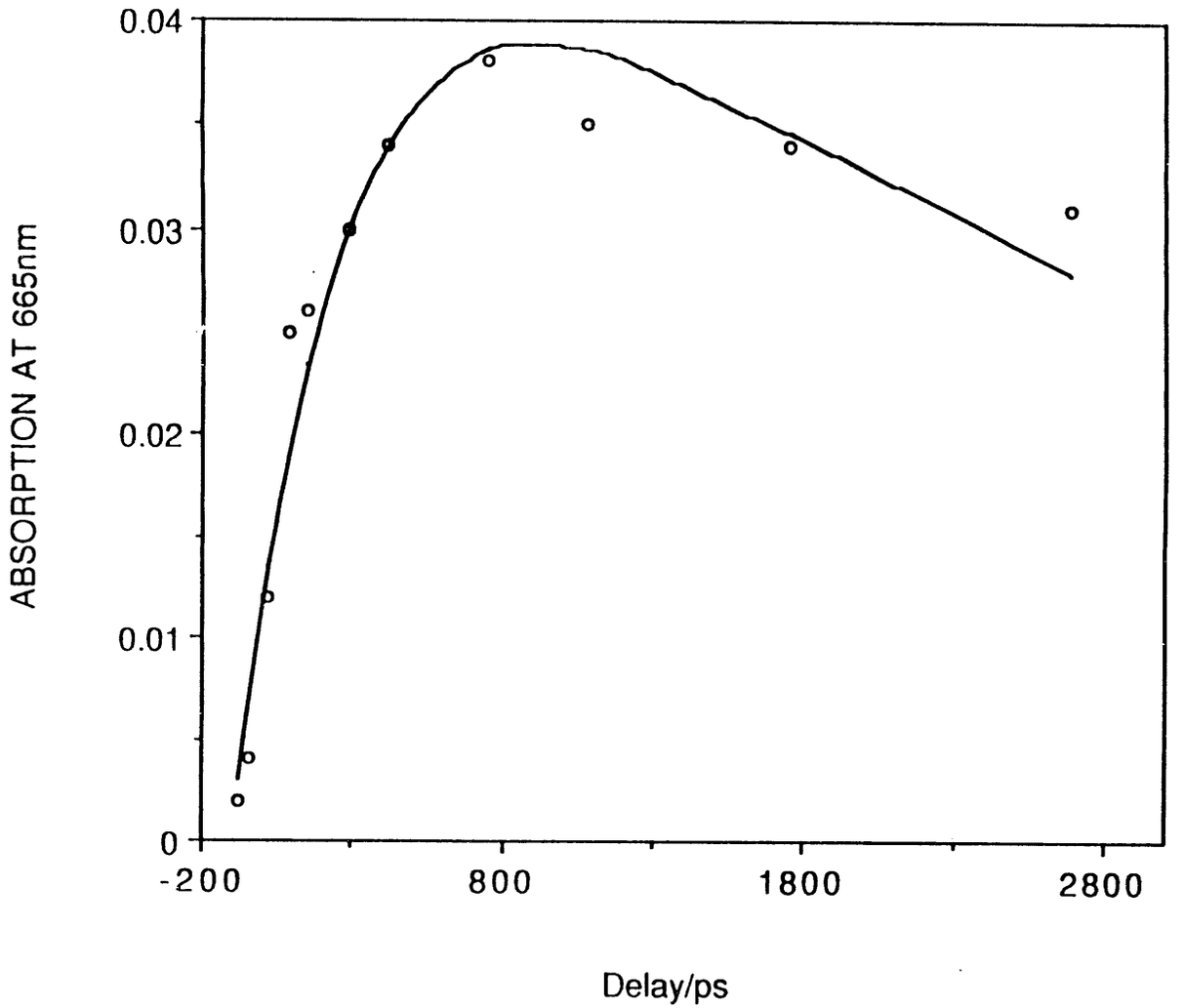

Figure 6b. PMA-DPA, pH=2.8, [MV2+]=80mM, fitted absorption rise.

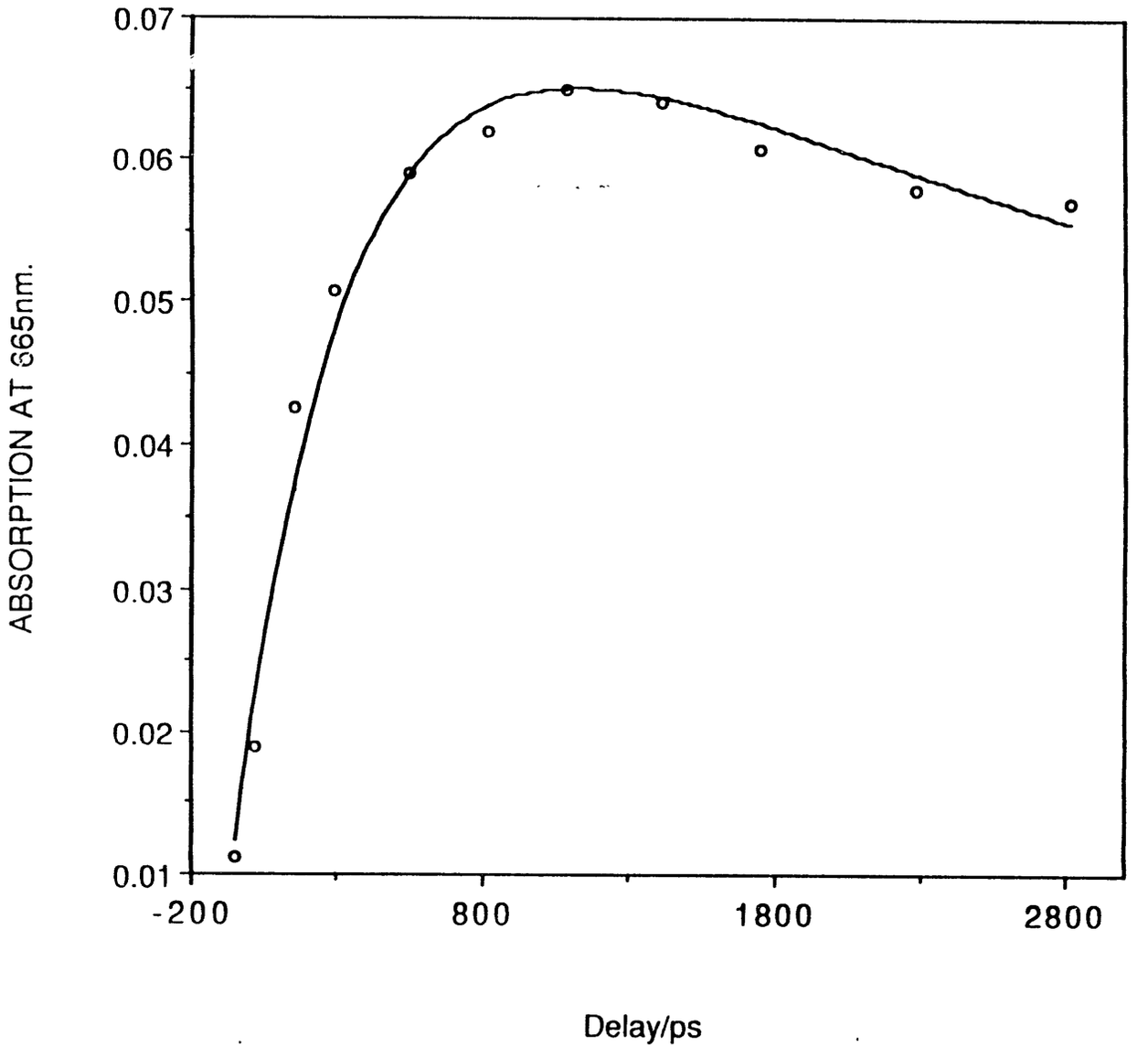

Table 2

$[MV^{2+}]$	$k_1 s^{-1}$	$k_2 s^{-1}$
40mM	$2.6(+/-0.8) \times 10^9$	$2.4(+/-1.1) \times 10^8$
80mM	$2.6(+/-0.51) \times 10^9$	$1.2(+/-0.46) \times 10^8$

In Table 2, k_1 represents the rate constant for the growth of the absorption at 665 nm and k_2 is the rate constant for the decay of the absorption. As the rate of growth of radical products is essentially independent of the concentration of quencher, this result suggests that the initial quenching mechanism is static in nature, probably occurring from a hydrophobically bound MV^{2+}. The singlet absorption of DPA decays with a rate constant of $2.24 \times 10^9 s^{-1}$, which is comparable to the rise of $MV^{+\bullet}$ absorption, indicating electron transfer occurs from the singlet state. The slight decay of the absorption on this time scale is unlikely to be diffusional in nature and is probably associated with a small degree geminate radical recombination according to the following scheme:

$$[\,(P)\text{–}{}^1DPA^{*} \;:\; MV^{2+}\,] \xrightarrow{k_1} [\,(P)\text{–}DPA^{+\bullet} \;:\; MV^{+\bullet}\,] \xrightarrow{k_{gr}} [\,(P)\text{–}DPA \;:\; MV^{2+}\,]$$

$$\downarrow k_{ce}$$

$$(P)\text{–}DPA^{+\bullet} + MV^{+\bullet}$$

where $[\,(P)\text{–}DPA \;:\; MV^{2+}\,]$ represents a bound complex in a solvent cage.

Previous work has shown that for PMA–DPA, charge separation only occurs at low pH, under which conditions the polymer is "hypercoiled," thus affording the chromophore some degree of hydrophobic protection. The above results are interpreted in terms of a loosely bound ground state complex between the DPA and viologen, which undergoes a photoinitiated electron transfer to form a loosely bound geminate ion pair, $(P)\text{–}DPA^{+\bullet} : MV^{+\bullet}$. This ion pair can then undergo charge recombination (k_{gr}) to form the initial reactants $(P)\text{–}DPA : MV^{2+}$, which is given by rate constant k_2, or charge escape (k_{ce}) to form solvated ions, which then undergo bimolecular recombination on the millisecond time scale.[2] The measured rate constant k_1 represents the rate constant for the reaction forming the initial ion pair, which has a rise time *ca* 400 ps. This means the rate of the forward electron transfer is not an instaneous process in this case. The forward rate could be slowed by the hypercoiling of PMA imposing some distance dependence on the

rate of electron transfer between the chromophore and MV^{2+}, or that some motion of the polymer coil is necessary to bring the redox centers into a more favorable position before electron transfer can occur.

PMA-DPA, pH = 9.0

Figure 7 shows the $S_1 \rightarrow S_n$ absorption of polymer-bound DPA under basic conditions. The absorption maximum appears to be blue-shifted by approximately 16 nm to 556 nm as compared to the S_1 absorption under acidic conditions. Addition of methylviologen to the solution results in immediate static quenching of $^1DPA^*$. This can be seen in Figure 8, which displays the time dependence of the singlet absorption at 556 nm. Quenching of the S_1 state occurs within our instrumental rise time resulting in an initially reduced yield of the singlet absorption. Subsequent decay of the residual S_1 absorption occurs as can be seen by inspection of Figure 8. However, the extent of decay is not sufficient, within our time window, to make good rate measurements. This will be investigated in more detail in future program years.

Figure 9 displays the absorption spectra for PMA–DPA/viologen system; no evidence for the formation of either $MV^{+\bullet}$ or $DPA^{+\bullet}$ is seen. This is in keeping with earlier work which found no evidence of radical species at this pH at sub-μs times.[2] Under basic conditions, the carboxylic acid backbone of the PMA is ionized and the polymer chain exists in an extended conformation in solution. The MV^{2+} is able to electrostatically bind to the carboxylate group, thus allowing the viologen to come into close contact with the chromophore.[3] This presumably allows a rapid reversible electron transfer to occur, which probably occurs in a few picoseconds. Mataga has shown that systems which form strong ground state charge-transfer complexes form contact ion-pairs which have been shown to have very short lifetimes.[4]

A short communication on this material has been published (Appendix V).

3.2.2 PMA-PY

Previous nanosecond studies have shown that PMA-PY does not form charge-separated products following quenching of pyrene S_1 at either high or low pH, unlike the analogous diphenyl-anthracene polymers.[5] These observations have been confirmed at the picosecond level with no evidence being found of charge separated products either at pH 2.8 or pH 9.0

PMA-PY, pH = 9.0

Figure 7 PMA-DPA, pH=9.0, singlet absorption.
Delays: (a) -46 (b) -13 (c) 20 (d) 2417ps

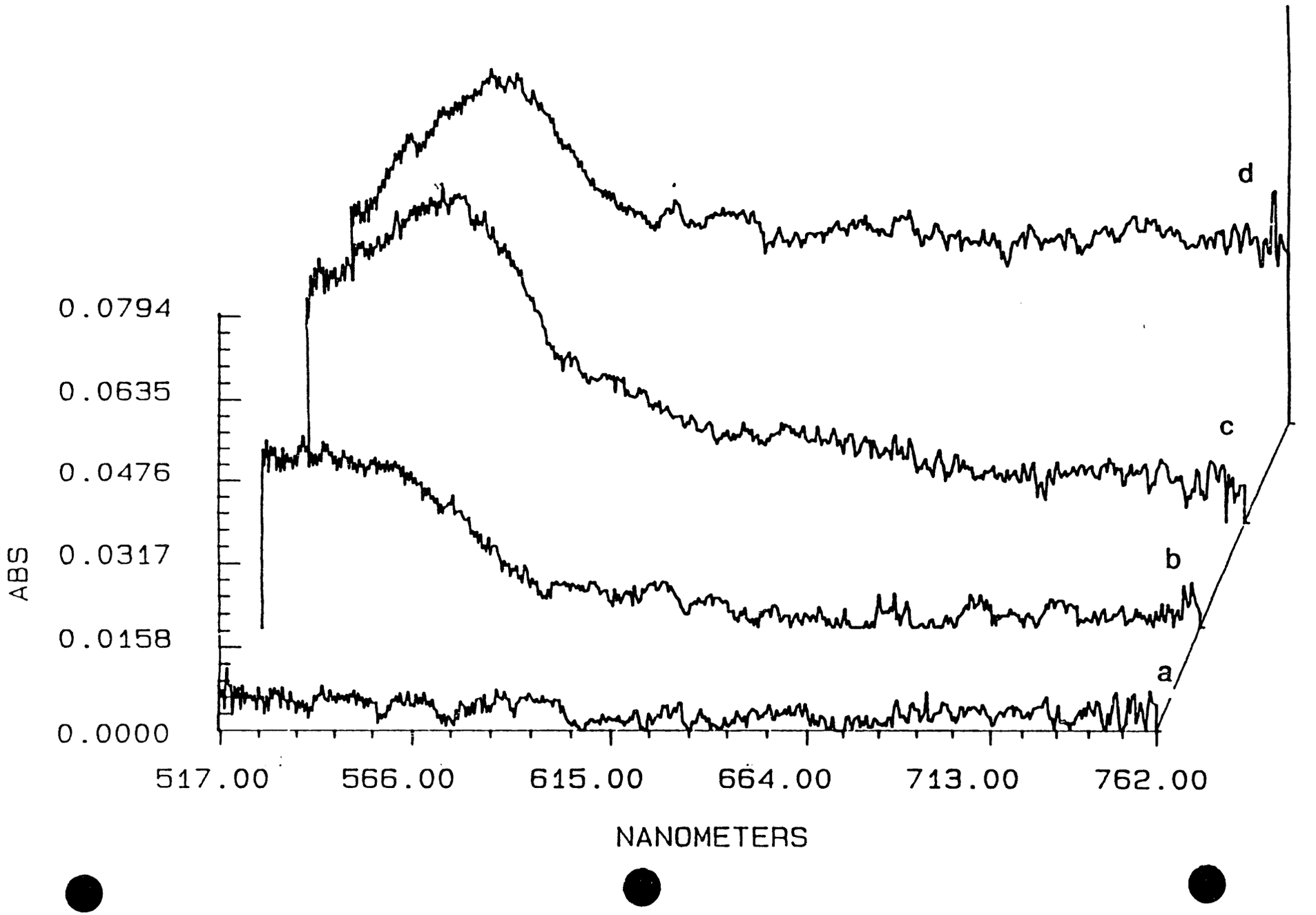

Figure 8. PMA-DPA, pH=9.0

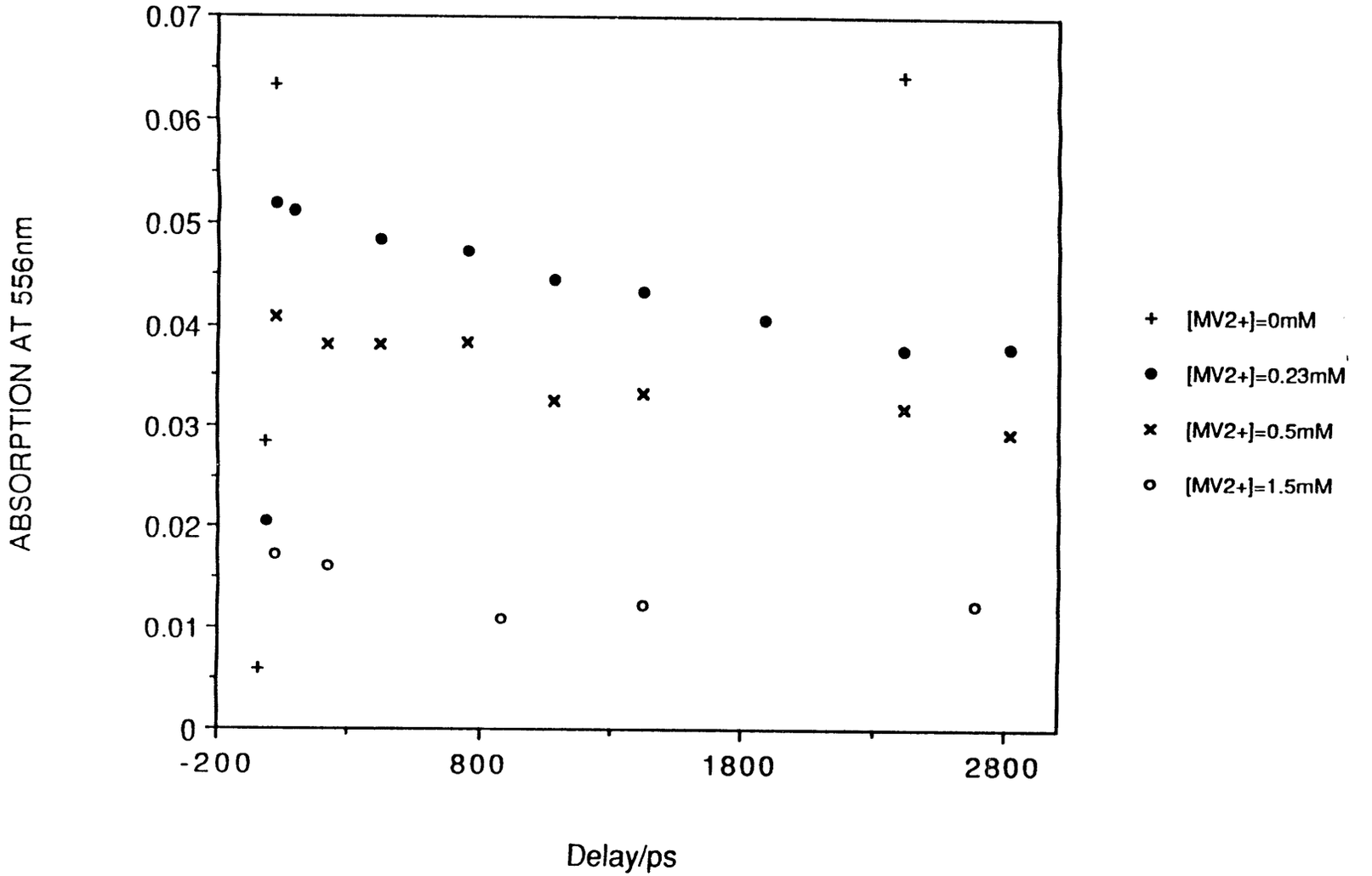

Figure 9. PMA-DPA, pH=9.00, [MV2+]=0.5mM
Delays: (a) 2817 (b) 1418 (c) 1085 (d) 20ps

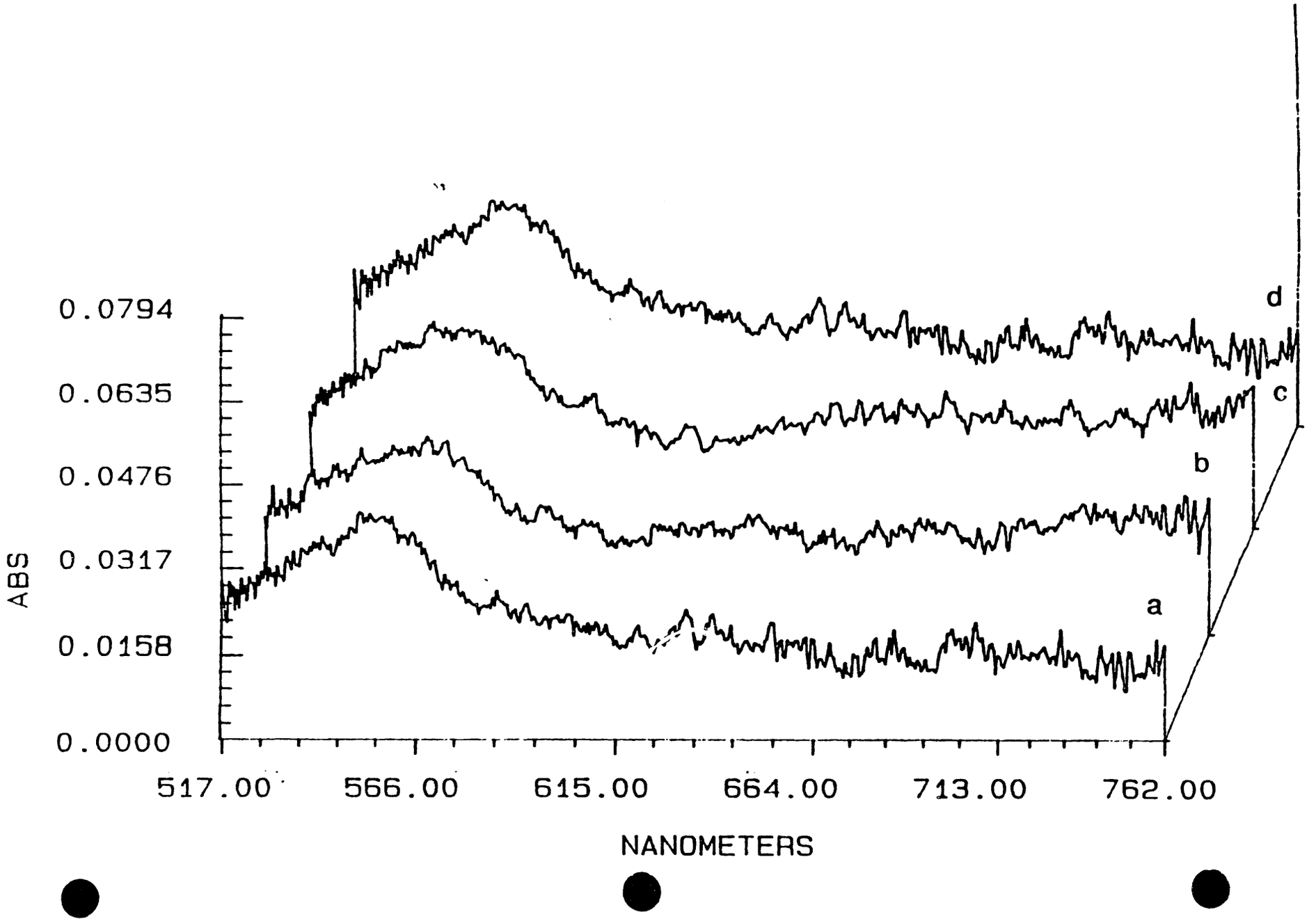

The polymer-bound pyrene has a singlet absorption maximum at ~482 nm and a shoulder at ~457 nm (Figure 10a), while free pyrene in ethanol solution has two well-defined peaks at 454 and 496 nm. Addition of MV^{2+} to the aqueous polymer solution (Figures 10b and 10c) results in a very efficient static quenching process similar to that seen with PMA-DPA at the same pH (see Figure 11), resulting in an instantaneous reduction of singlet absorption with no redox-separated products being observed. In this, PMA-PY follows the PMA-DPA discussed above.

PMA-PY, pH = 2.8

The singlet absorption spectrum of PMA-PY at pH = 2.8 (see Figure 12) is broadened compared to that at high pH, with a maximum at 477 nm and a shoulder at 504 nm. Addition of MV^{2+} again results in no redox separated products as with pH 9.0 (see Figure 13). Figures 14a and 14b display the absorption at 473 nm ($S_1 \rightarrow S_n$ maximum) and 620 nm ($MV^{+\bullet}$) respectively, with and without added MV^{2+}. Examination of these figures reveals that while the singlet state of pyrene is being quenched, there is no increase in absorption at 620 nm due to $MV^{+\bullet}$.

The major difference between the pyrene and DPA system is the presence of strong ground-state complexation between chromophore and MV^{2+} at both high and low pH. This means that hydrophobic protection of pyrene by the polymer coil at low pH is significantly reduced compared to that of the DPA system. This allows a close approach of donor and acceptor, which are then able to form a contact ion-pair. The differences in the degree of hydrophobic protection between the two systems could be related to a number of factors; namely: the structure of pyrene could disrupt the hypercoiling of PMA, or the phenyl groups at the 9,10 positions of DPA could somehow prevent the close approach of MV^{2+}.

PMA-PY, pH = 4.0

PMA-PY shows similar results to those seen at pH 2.8.

4.0 Final Program Year

Although much interesting research on the tagged polymers was left undone at the end of the second program year, it was decided to switch gears and enter another area. The major reason for this was that the manufacture of the polymer-bound chromophores relied upon expertise that existed within the Webber laboratory in Texas. The emphasis there had changed and the systems were no

Figure 10a

PMA-PY, pH=9.0, singlet absorption

Delays: (a) -80 (b) 20 (c) 1418 (d) 2817ps

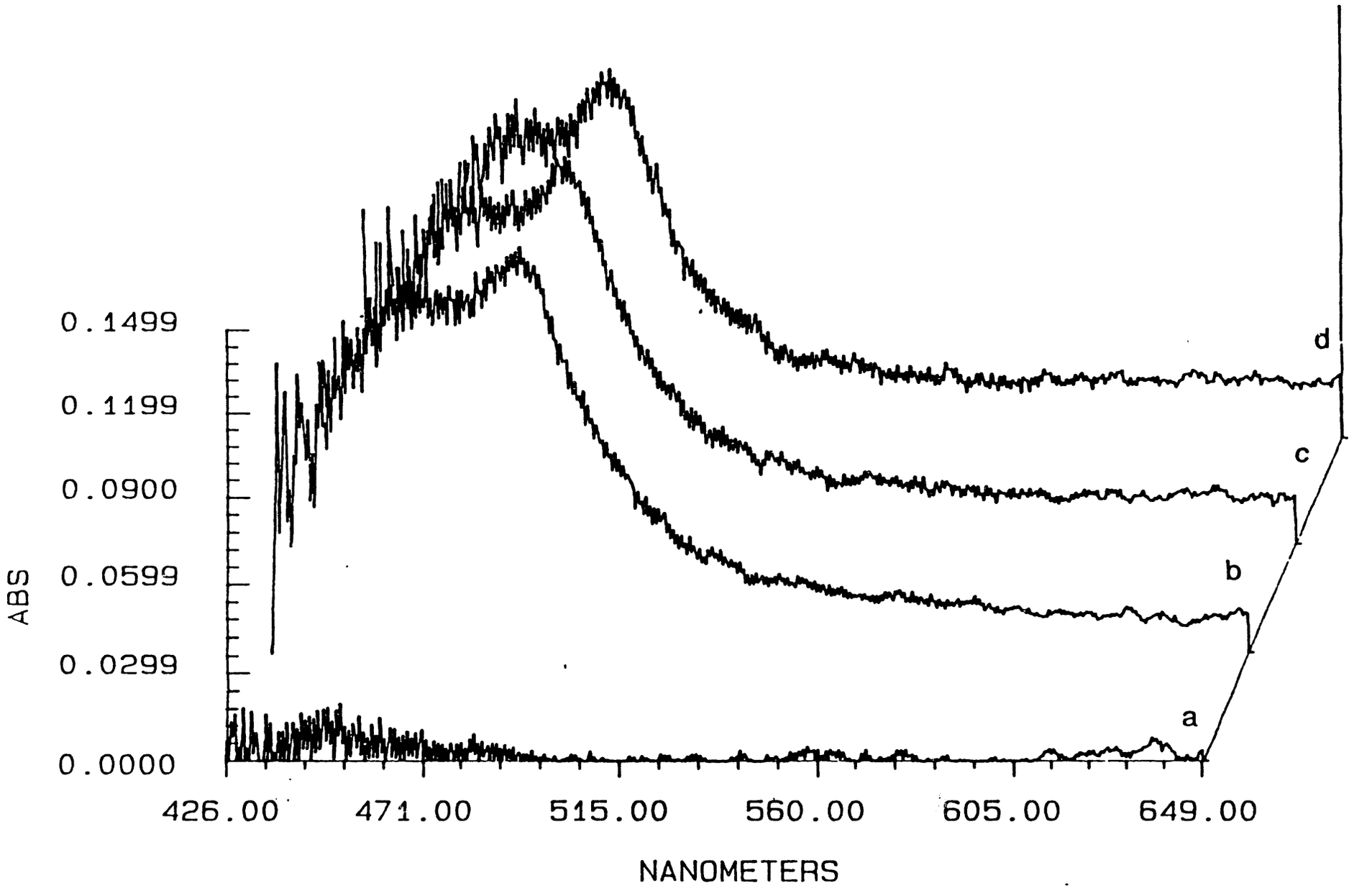

Figure 10b PMA-PY, pH=9.0, [MV2+]=0.1mM
Delays: (a) -46 (b) 2817 (c) 1418 (d) 20ps

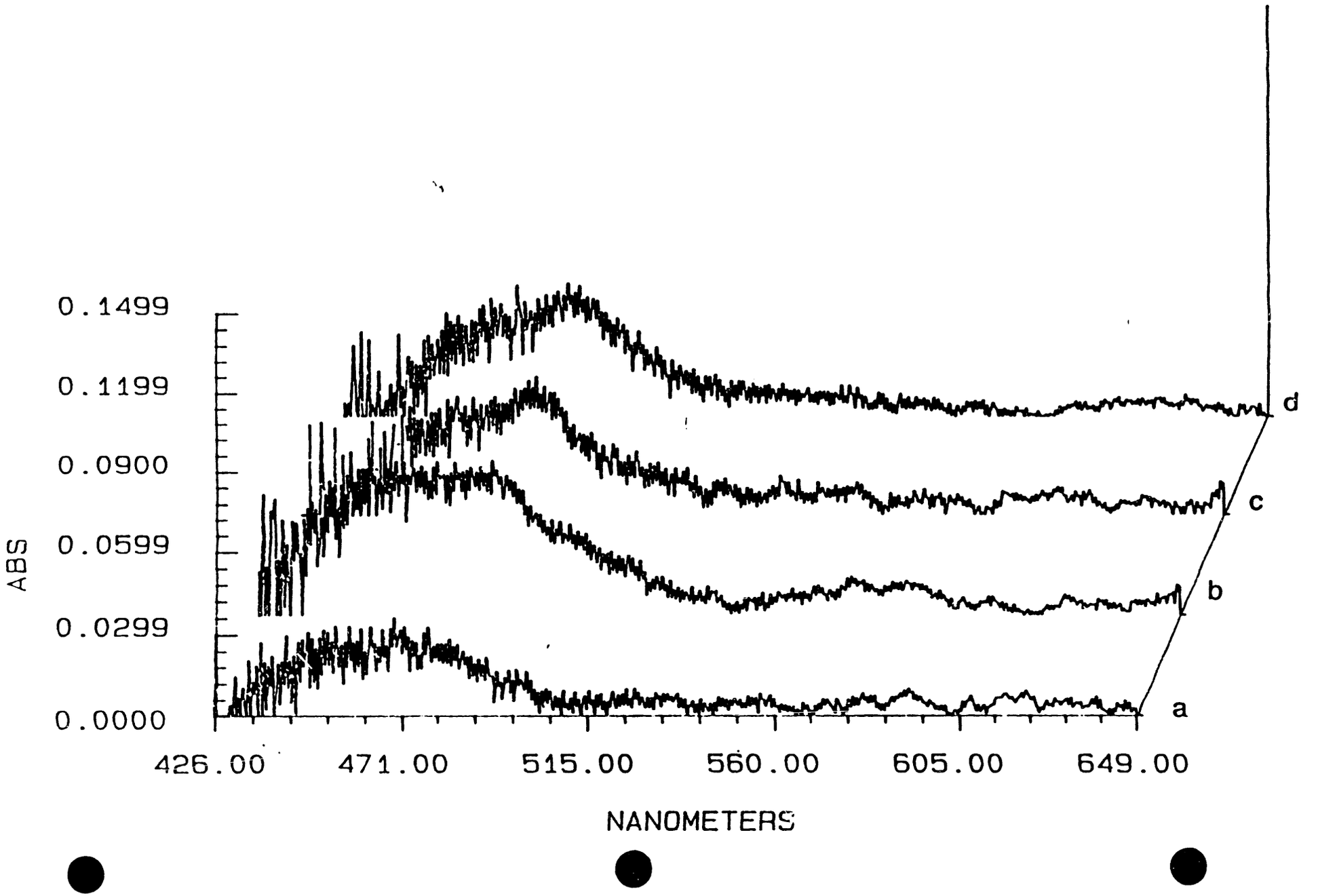

Figure 10c PMA-PY, pH=9.0, [MV2+]=0.2mM

Delays: (a) 2817 (b) 1418 (c) 20ps

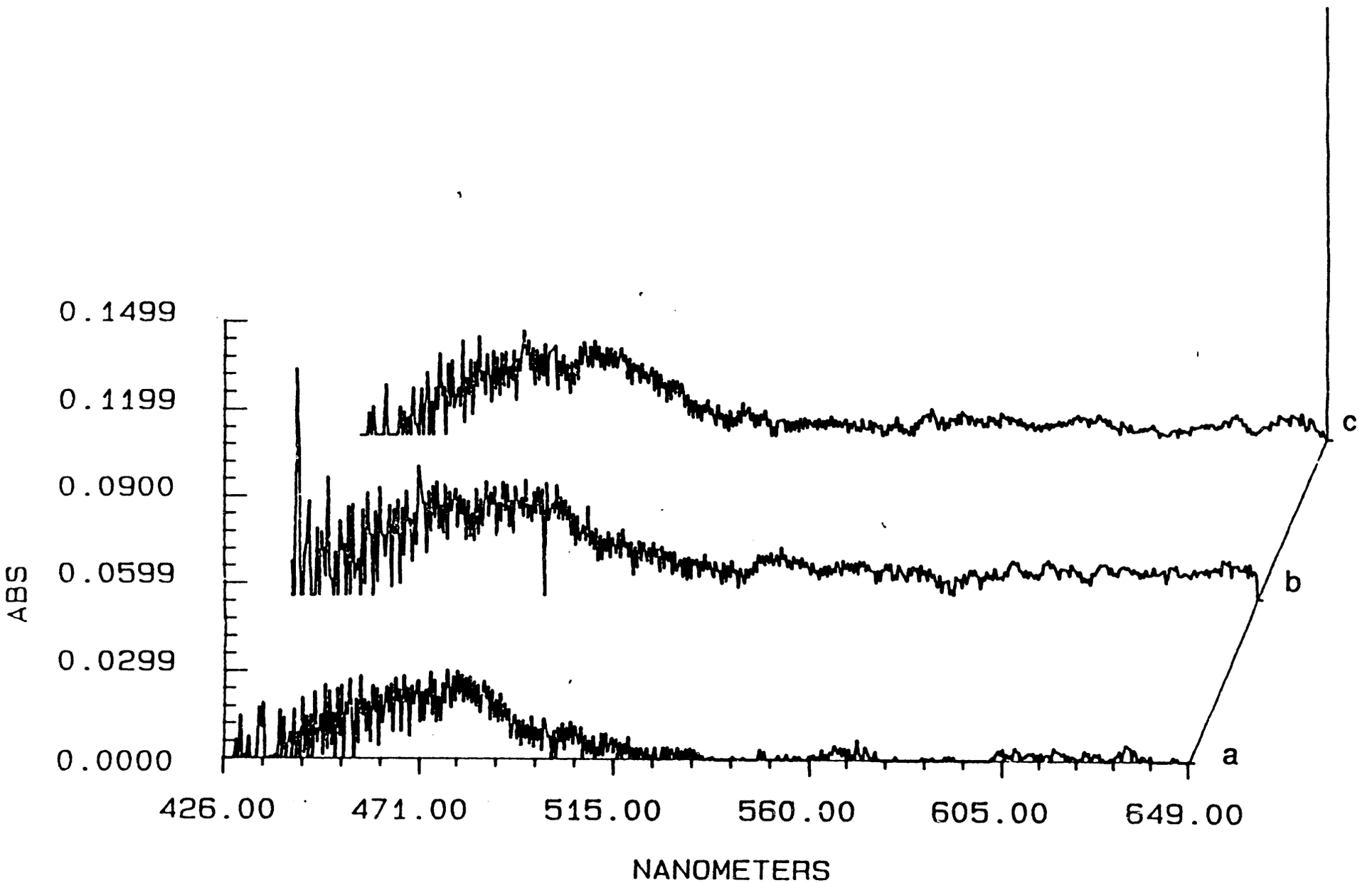

Figure 11. PMA-PY, pH=9.0. Decay of singlet absorption at 486nm.

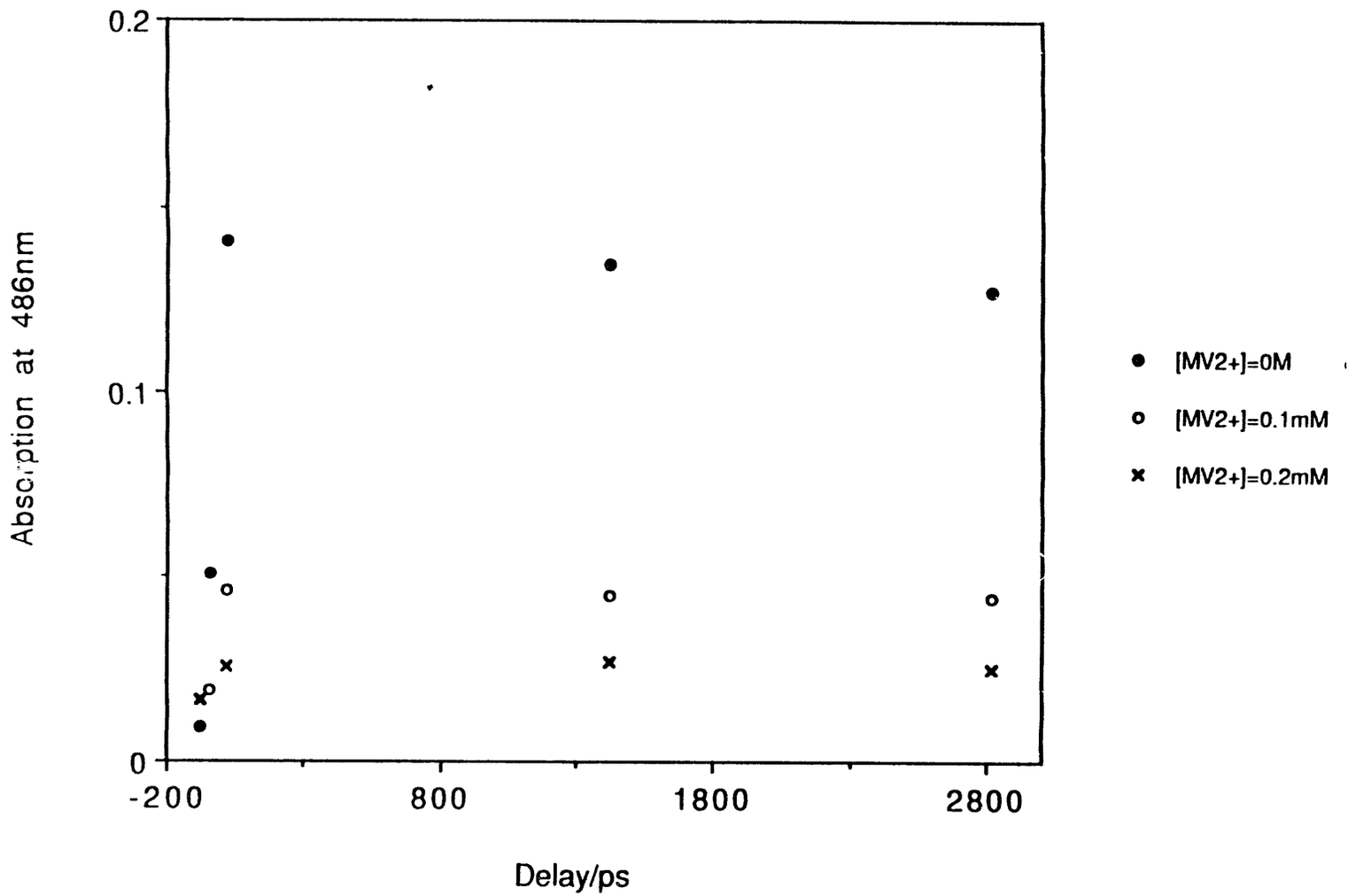

Figure 13 PMA-PY, pH=2.8, [MV2+] =40mM

Delays: (a) -113 (b) 2684 (c) 1085 (d) 20ps

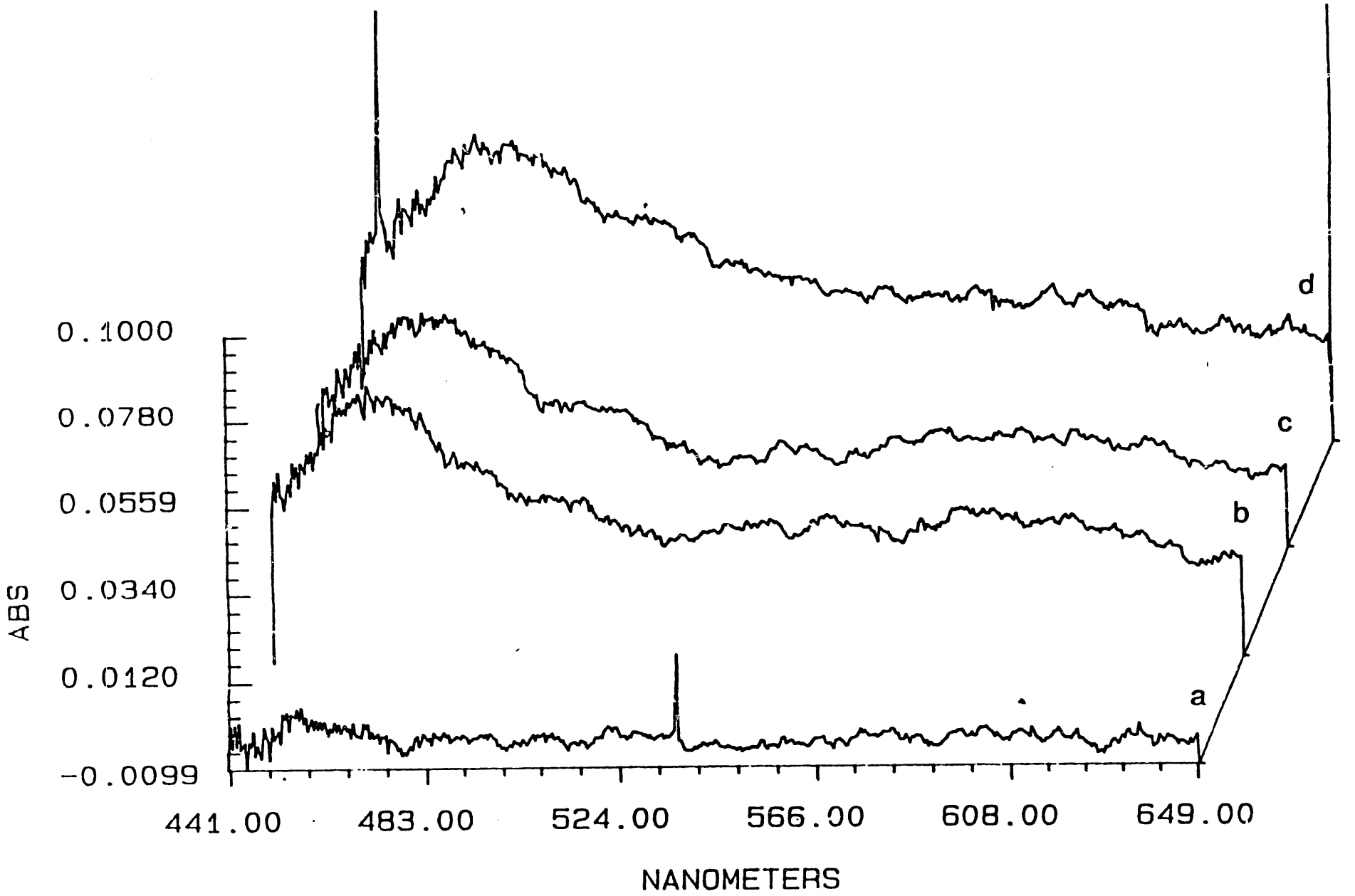

Figure 14a. PMA-PY, pH=2.8, absorption at 473nm.

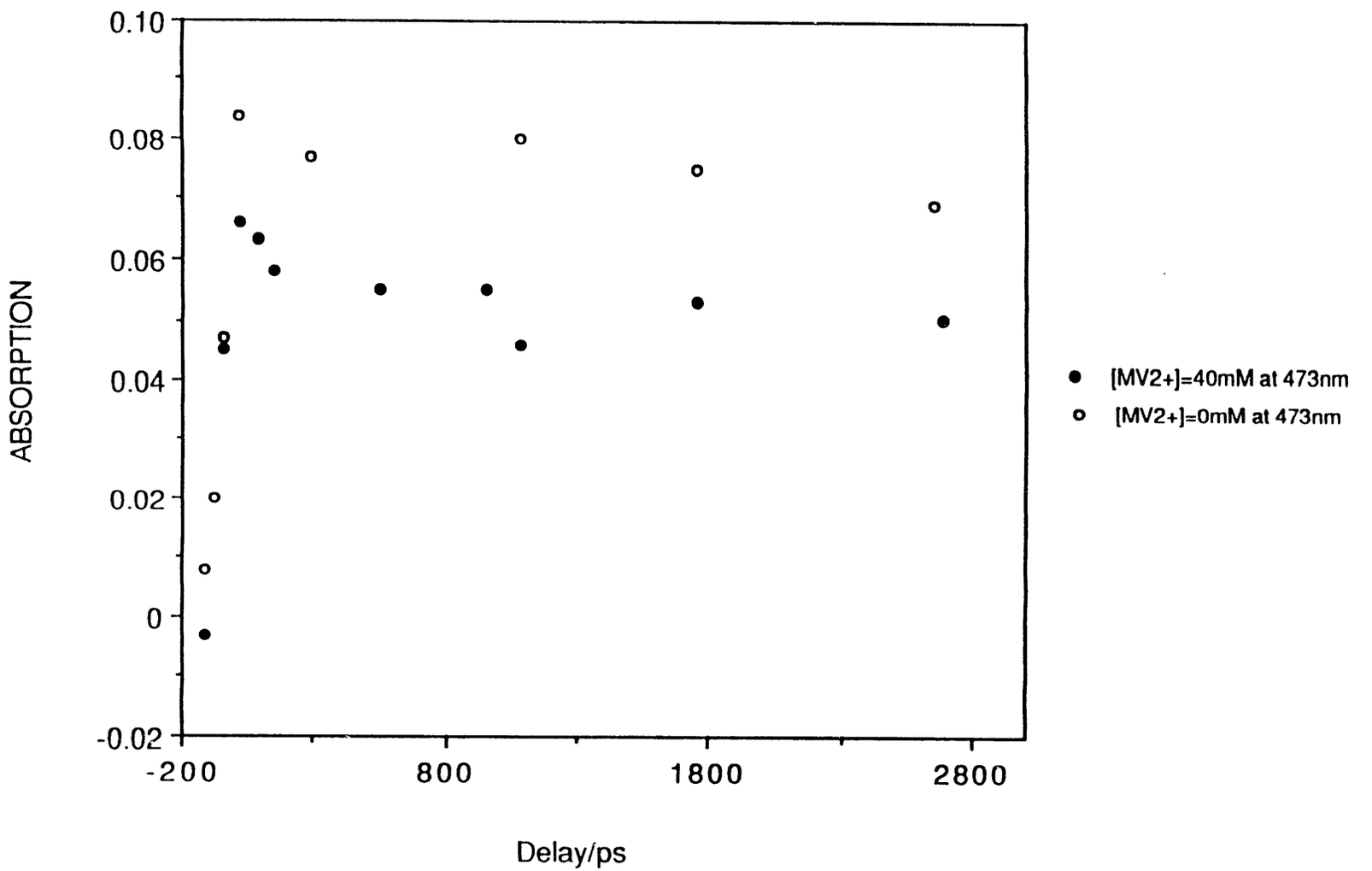

Figure 14b. PMA-PY, pH=2.8, absorption at 620nm

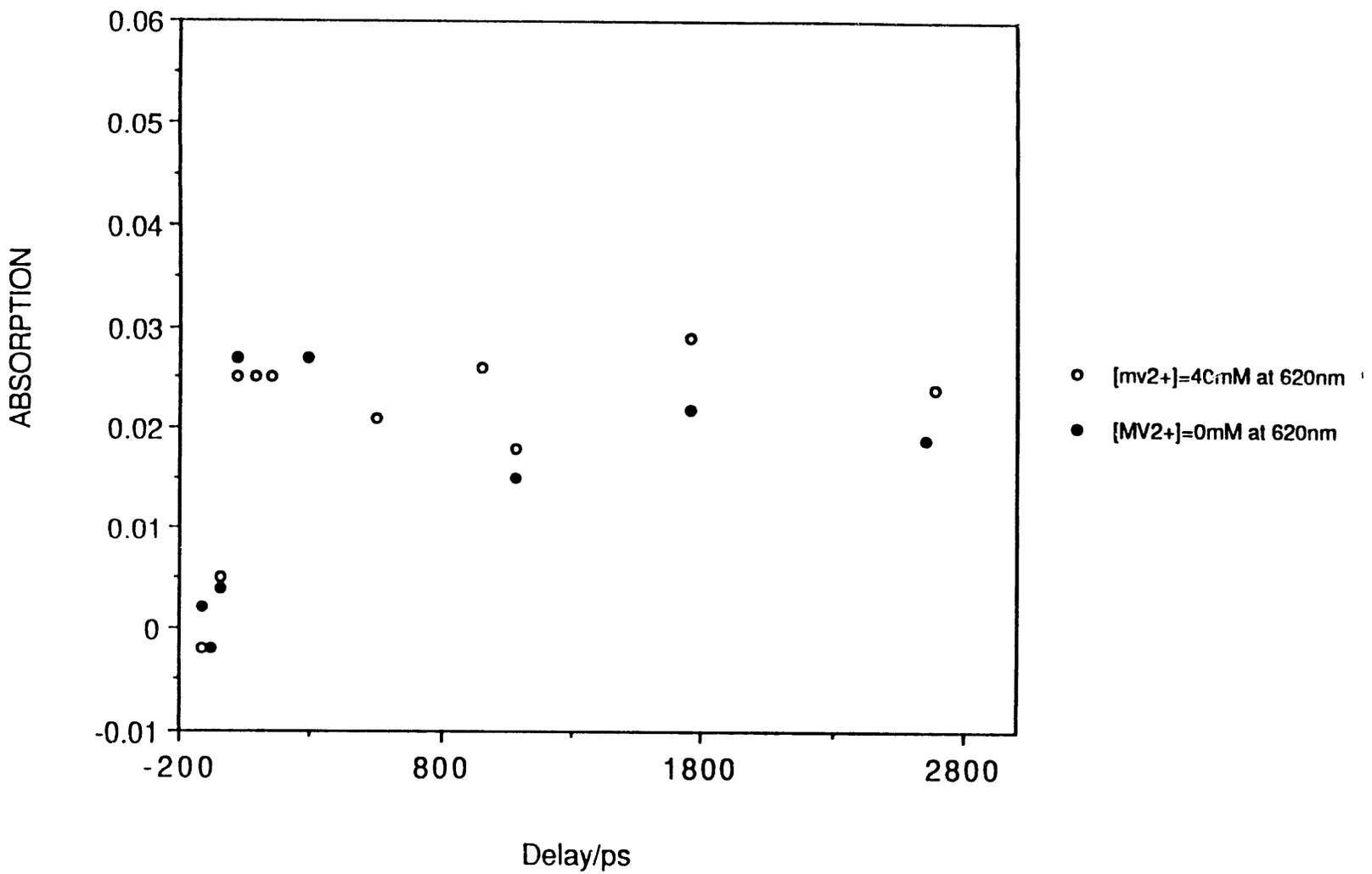

longer being synthesized. No relevant experience existed in the Bowling Green group, and the magnitude of the DOE grant did not allow for the hiring of a polymer synthesis expert. In light of these factors, it was decided to investigate photoredox reactions involving Ru(II) polypyridine complexes and some water-soluble aromatic materials.

4.1 Energy and Electron Transfer Reactions involving $[Ru(bipy)_3]^{2+}$ and Aromatic Chromophores

We are interested in developing new lipid bilayer systems for artificial photosynthesis. Our approach to studying light-initiated energy and electron transfer reactions in these systems is to utilize a Ru(II)polypyridine complex as the primary chromophore and aromatic molecules such as acridine or pyrene as secondary chromophores, whose triplet states are sensitized by the Ru(II) complex. Several features of the Ru(II)polypyridine chromophore make it attractive for use as a sensitizer in model photosynthetic systems. These complexes absorb over a wide range of the visible spectrum, including 532 nm, so that they can be excited with the second harmonic of the Nd:YAG laser. This feature is important for the research program because it makes it possible to selectively excite Ru(II)polypyridine as the primary chromophore without exciting the secondary chromophores. The Ru(II) complexes rival organic ketones as triplet state photosensitizers in that intersystem crossing occurs with essentially 100% efficiency and an energy loss of only a few kilocalories per mole.[6-10] The lowest excited state, which is largely triplet in character, luminesces in fluid solution. This makes it possible to monitor the kinetic behavior of the excited state directly, without interference from other transients. The complexes are resistant to photodegradation, which makes it possible to subject them to multiple laser shots for signal averaging purposes during laser flash photolysis experiments without altering their composition and kinetic behavior. Furthermore, Ru(II)polypyridine complexes have relatively little tendency to undergo self-quenching in the excited state as a result of ground-state aggregation or reaction between the ground and excited state molecules.[11-14] This property is especially important for studies with colloidal media such as lipid bilayers, where the local concentration of the photosensitizer in the dispersed phase can be high.

The advantageous photophysical properties of Ru(II)polypyridine complexes as triplet sensitizers, such as the efficient intersystem crossing and conservation of photon energy already mentioned, arise in part from the fact that spin-orbit coupling induced by the metal ion introduces a certain degree of singlet

and triplet character into the lowest excited state. Spin-orbit coupling is also responsible, however, for a relatively short excited state lifetime (*ca* 1 μs) and, frequently, inefficient charge separation following excited state redox quenching.[15-16] In recent years, several research groups have shown that anthracene and its derivatives can dramatically enhance the quantum efficiency of photoredox reactions that are initiated by Ru(II)polypyridine complexes.[15,17,18] In these systems, energy transfer from the photoexcited Ru(II) chromophore to the anthracene chromophore produces the anthracene triplet, which subsequently sensitizes electron transfer from donor to acceptor. The addition of anthracene as an energy relay improves the efficiency of photoconversion because its triplet state is longer-lived and generates free radical products more efficiently than the Ru(II) complex alone.[15,17-21] We recently extended this approach to the acridine, phenazine, and pyrene chromophores using $[Ru(bipy)_3]^{2+}$ (bipy ≡ 2,2'-bipyridine) as the photosensitizer.

Our experimental results dealing with the photosensitization of the triplet states of acridine and phenazine by $[Ru(bipy)_3]^{2+}$ as well as the redox chemistry of the acridine triplet were published recently (see Appendices VI and VII). This section summarizes our more recent results with pyrene-1-butyric acid (PBA). Triplet-triplet (T-T) energy transfer from Ru(II)polypyridine to pyrene has not been reported previously in the literature. The triplet state energy (E_T) of pyrene, 48 kcal/mole,[22] is about 1 kcal/mole less than that of $[Ru(bipy)_3]^{2+}$, so that T-T energy transfer is slightly exothermic. The butyric acid substitution of pyrene lowers its E_T by *ca* 0.5 kcal/mole.[23] The bimolecular rate constants for energy transfer from $[Ru(bipy)_3]^{2+}$ to PBA aqueous methanol (10 vol% water) containing either 0.1 M NH_4HCO_3 or 0.1 M CH_3COOH are 6.7×10^9 $M^{-1}s^{-1}$ and 2.6×10^9 $M^{-1}s^{-1}$, respectively. Thus intermolecular T-T energy transfer occurs with near the diffusion-controlled rate despite the fact that the driving force is only 1-2 kcal/mole.

The redox chemistry of the triplet state of PBA ($^3PBA^*$) was examined with aqueous methanol (10 vol% water) and 0.1 M NH_4HCO_3 as the solvent. The triplet was generated either by photosensitization with $[Ru(bipy)_3]^{2+}$ or by direct photoexcitation (355 nm). The lifetime in deaerated solution is *ca* 200 μs. In contrast to acridine-9-carboxylate, $^3PBA^*$ is readily quenched by MV^{2+} ($k = 1.0 \times 10^{10}$ $M^{-1}s^{-1}$), but not by phenols. Transient absorption measurements show that quenching by MV^{2+} occurs

via electron transfer from $^3PBA^*$. The spectra in Figure 15 show the conversion of $^3PBA^*$ (λ_T^{max} = 415 nm, see Inset) and MV^{2+} into the semioxidized radical of PBA ($PBA^{+\cdot}$, λ_{max} = 460 nm) and the semireduced radical of MV^{2+} ($MV^{+\cdot}$, λ_{max} = 395 nm). The growth of $MV^{+\cdot}$, monitored at either 395 nm or 602 nm, parallels the decay of the triplet and establishes the fact that electron transfer occurs via triplet-state rather than singlet-state quenching. The $PBA^{+\cdot}$ and $MV^{+\cdot}$ that are produced subsequently decay by processes that include recombination, but the $PBA^{+\bullet}$ decays at a faster rate than $MV^{+\cdot}$, indicating that it may be reacting with the solvent or undergoing disproportionation. The molar extinction coefficient of $PBA^{+\cdot}$ is not known with certainty at this time, but it is probably within the range of (1–2) x 10^4 $M^{-1}cm^{-1}$. The yield of $MV^{+\cdot}$ per quenched $^3PBA^*$ is estimated to be at least 80%.

Phenols such as vitamin E analogues and 4-hydroxybenzoate ($HOPhCOO^-$) reduce $PBA^{+\cdot}$ subsequent to electron transfer from $^3PBA^*$ to MV^{2+}. The rate constant for the reduction of $PBA^{+\cdot}$ by $HOPhCOO^-$ is *ca* 2 x 10^8 $M^{-1}s^{-1}$. Figure 16 shows the transient absorption spectra that are obtained in the absence and presence of $HOPhCOO^-$. The phenoxyl radical derived from $HOPhCOO^-$ ($\lambda_{max} \cong$ 425 nm, $\varepsilon \cong$ 1,200 $M^{-1}cm^{-1}$)[24] does not absorb strongly enough in this spectral region compared to $MV^{+\cdot}$ (ε = 42,000 $M^{-1}cm^{-1}$ at 395 nm[25]) to be evident. The inset in Figure 16 is the spectrum attributed to $PBA^{+\cdot}$ that is obtained by subtracting the transient spectrum observed with added $HOPhCOO^-$ from that observed without it. This spectrum resembles that reported for the radical cation of pyrene.[26,27] The $MV^{+\cdot}$ and phenoxyl radicals recombine with a rate constant of *ca* 4 x 10^9 $M^{-1}s^{-1}$.

The results with the acridine and pyrene triplets reveal their contrasting reactivities toward electron donors and acceptors. While the acridine triplet is quenched by phenols to give semireduced acridine ("reductive quenching"), it is unreactive towards MV^{2+}. On the other hand, the pyrene triplet is quenched by MV^{2+} to give semioxidized pyrene ("oxidative quenching"), but it does not react with phenols. Anthracene resembles pyrene in this respect. Thus it is possible with these chromophores to photosensitize the same electron transfer reaction by either a reductive or oxidative quenching pathway. These reactions can be sensitized with visible light using Ru(II)polypyridine as the primary chromophore.

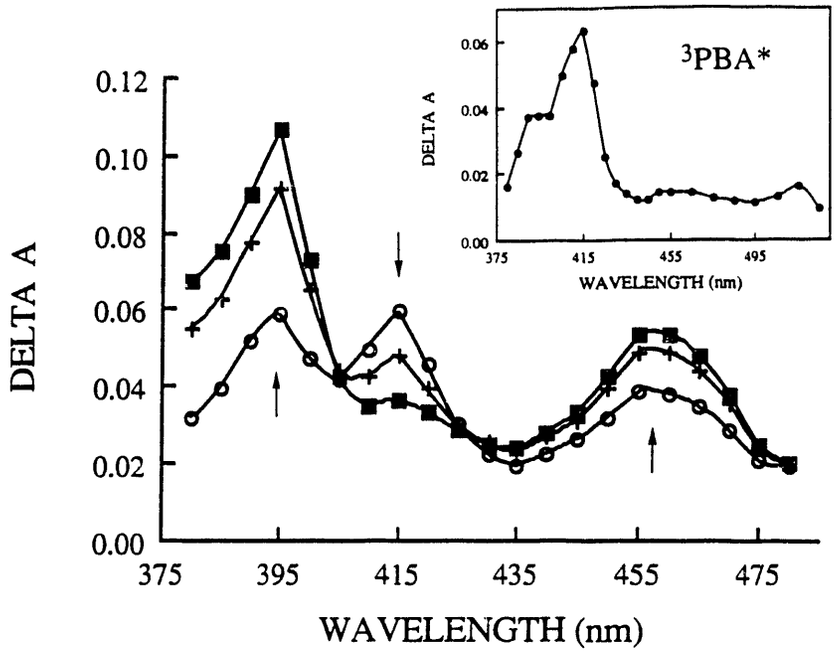

FIGURE 15: Time-resolved difference absorption spectra demonstrating electron transfer from ^{3}PBA* to MV^{2+}. The spectra were obtained 2, 3, 5, and 9 μs after 355-nm laser excitation. INSET: The spectrum of ^{3}PBA* obtained in the absence of MV^{2+}. The solvent is deaerated methanol containing 10 vol% water and 0.1 M NH_4HCO_3.

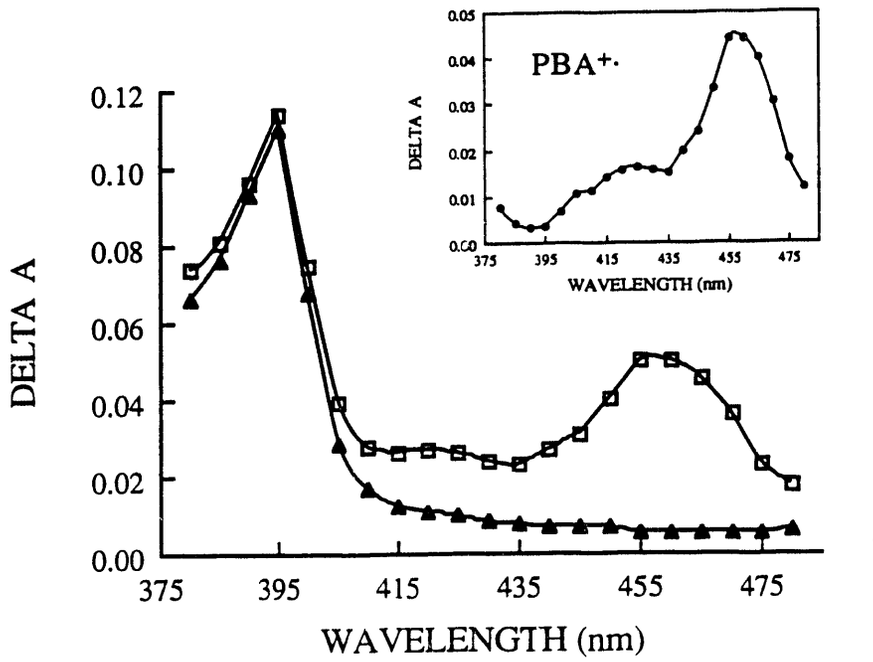

FIGURE 16: Difference absorption spectra of the products following electron transfer from ^{3}PBA* to MV^{2+} in the absence or presence of $HOPhCOO^-$ (0.42 mM) as electron donor. INSET: The spectrum of $PBA^{+\cdot}$ obtained by subtracting the spectra obtained with and without $HOPhCOO^-$. The solvent is the same as in Figure 15.

5.0 Summary and Conclusions

The early studies showed clearly that in all cases, polymer-bound chromophore fluorescence was quenched by viologen electron acceptor species; the kinetics of quenching was often complex, and a strong pH dependence was noted. Kinetic spectrophotometric observations at sub-microsecond times showed quantum yields of radical ion pair formation varying from 0 through 0.45 depending on the nature of the chromophore and the pH. The later sub-nanosecond absorption experiments revealed that, for those systems studied, charge separation was high at pH = 2.8 for PMA-DPA and the other anthracenes, tending to zero at pH = 9. The copolymer PMA-PY had zero tendency to show any charge separation at any pH, the results lending themselves to an interpretation involving severe static quenching.

Interestingly, the rate of formation of the ion pair species in PMA-DPA indicated a formation time of *ca* 400 ps and a subsequent decay with *ca* 4 ns lifetime. The latter value, which is tentative only, because of the short time window we have available, indicates that rapid geminate decay of the ion pair must be competing with long term (μs) cage escape since our longer time studies showed escape yields of 0.4 or so. The 400 ps rise time is perhaps a reflection of the distance across which the electron transfer must occur, or maybe shows a Marcus inverted region effect.

In the Ru(II)polypyridine phase of the program, it was shown that acridine triplets, formed by energy transfer from the photoexcited Ru(II) complexes, undergo reductive quenching with phenolic materials. On the other hand, pyrene triplets, formed similarly, are quenched by MV^{2+} to yield reduced viologen species.

BIBLIOGRAPHY

1. Declemy, A. and C. Rulliere (1986) *Rev. Sci. Instrum.* **57**, 2733.

2. Stramel, R. D., M. A. J. Rodgers, S. E. Webber (1989) *J. Phys. Chem.* **93**, 1928.

3. Delaire, J. A., M. A. J. Rodgers, S. E. Webber (1984) *J. Phys. Chem.* **88**, 6219.

4. Tsuyoshi, A. and N. Mataga (1989) *J. Phys. Chem.* **93**, 6575.

5. Stramel, R. D., C. Nguyen, S. E. Webber, M. A. J. Rodgers (1988) *J. Phys. Chem.* **92**, 2934.

6. V. Balzani, F. V, M. T. Gandolfi, and M. Maestri (1978) *Top. Curr. Chem.* **75**, 1-64.

7. K. Kalyanasundaram (1982) *Coord. Chem. Rev.* **46**, 159-244.

8. R. J. Watts (1983) *J. Chem. Educ.* **60**, 834-842.

9. G. J. Kavarnos and N. J. Turro (1986) *Chem. Rev.* **86**, 401-449.

10. R. Krause (1987) *Structure and Bonding* **67**, 1-52.

11. G. L. Gaines, Jr., P. E. Behnken, and S. J. Valenty (1978) *J. Am. Chem. Soc.* **100**, 6549-6559.

12. W. Shi, S. Wolfgang, T. C. Strekas, and H. D. Gafney (1985) *J. Phys. Chem.* **89**, 974-978.

13. N. A. Surridge, S. F. McClanahan, J. T. Hupp, E. Danielson, S. Gould, and T. J. Meyer (1989) *J. Phys. Chem.* **93**, 294-304.

14. J. N. Younathan, S. F. McClanahan, and T. J. Meyer (1989) *Macromolecules* **22**, 1048-1054.

15. J. Olmsted III and T. J. Meyer (1987) *J. Phys. Chem.* **91**, 1649-1655.

16. U. E. Steiner, H.-J. Wolff, T. Ulrich, and T. Ohno (1989) *J. Phys. Chem.* **93**, 5147-5154.

17. O. Johansen, A. W.-H. Mau, and W. H. F. Sasse (1983) *Chem. Phys. Lett.* **94**, 113-117.

18. J. Olmsted III, S. F. McClanahan, E. Danielson, J. N. Younathan, and T. J. Meyer (1987) *J. Am. Chem. Soc.* **109**, 3297-3301.

19. P. K. Das (1983) *J. Chem. Soc., Faraday Trans. 1* **79**, 1135-1145.

20. O. Johansen, A. W.-H. Mau, and W. H. F. Sasse (1983) *Chem. Phys. Lett.* **94**, 107-112.

21. Y. Usui, Y. Sasaki, Y. Ishii, and K. Tokumaru (1988) *Bull. Chem. Soc. Jpn.* **61**, 3335-3337.

22. I. Carmichael and G. L. Hug (1989) "Spectroscopy and intramolecular photophysics of triplet states," In J. C. Scaiano (ed.) *Handbook of Organic Photochemistry*, Vol. I, CRC Press, Boca Raton, FL, Chap. 16, pp 369-403.

23. M. Skrilec and L. J. Cline Love (1980) *Anal. Chem.* **52**, 1559-1564.

24. J. Lind, X. Shen, T. E. Eriksen, and G. Merenyi (1990) *J. Am. Chem. Soc.* **112**, 479-482.

25. T. Watanabe and K. Honda (1982) *J. Phys. Chem.* **86**, 2617-2619.

26. H. Hiratsuka and Y. Tanizaki (1979) *J. Phys. Chem.* **83**, 2501-2505.

27. T. Shida (Editor) (1988) *Electronic Absorption Spectra of Radical Ions*, Elsevier Science Publishers, New York.

Appendices 1-7 removed and cycled separately —

END

DATE
FILMED
11 122191